Vaccination and transportation intervention strategies for effective pandemic control

Abstract

The COVID-19 pandemic highlighted the pivotal role of transportation-related controls and vaccination in mitigating widespread infections. However, the substantial costs associated with these interventions necessitate a nuanced equilibrium between control measures and infection risks. This study, driven by the recognition of spatial heterogeneities in mobility networks and epidemic vulnerability, presents an optimal control framework for two control measures—vaccine distribution and transportation restrictions—within a metapopulation structure. The overarching goal is to minimize the total costs derived from the implementation of control measures and health and opportunity loss from infection. Our findings highlight the effectiveness of transportation control and vaccine distribution in reducing both total costs and infection rates. Notably, the efficacy of these control measures exhibits regional variations, and the simultaneous implementation of both measures emerges as the most effective and economically viable strategy. The synergy effect between vaccine distribution and transportation restrictions is also a key observation in our simulations, showcasing their complementary roles in pandemic control. By considering the spatial nuances of mobility networks and infection vulnerability, this framework provides a flexible and region-specific strategy to optimize the allocation of resources for pandemic control, ultimately striking a balance between efficacy and economic feasibility.

Keywords: COVID-19 Pandemic, Transportation and vaccination control, Metapopulation model, Cost minimization

1. Introduction

The emergence of the COVID-19 pandemic in December 2019 swiftly evolved into a global crisis, necessitating rapid and widespread interventions to curb its dissemination. Early non-pharmaceutical interventions, such as travel restrictions, played a crucial role in controlling the virus's spread (UNWTO, 2020). As vaccines were developed and distributed globally, there was a gradual easing of those interventions, allowing public to return to normalcy in daily life and travel patterns.

Transport-related control policies were among the initial strategies adopted to combat the pandemic. Transportation restrictions are measures aimed at controlling the movement of people between various locations, including travel bans, quarantine mandates, reduced public transportation services, or the closure of transportation hubs like airports or train stations (Zhang et al., 2021). These restrictions are implemented to curtail the spread of infectious diseases by limiting the mobility of potentially infected individuals across different areas. With the widespread transportation restriction policies, the effectiveness of mitigating and delaying the virus's transmission was observed through the reduced long-distance and short-range mobility (Chinazzi et al., 2020; Zhang et al., 2021). Notable successes include the substantial reduction in confirmed cases through lockdown policies in China and the risk mitigation achieved by the declaration of a state of emergency (SoE) in Japan (Murano et al., 2021; Hale et al., 2022). Despite these successes, the economic toll of travel restrictions, particularly on the tourism and aviation industry, was profound and necessitated a balance of transportation recovery and infection control (Dube et al., 2021). Simultaneously, significant global investments in medical research and development led to the approval of COVID-19 vaccines for emergency use in many countries (Ndwandwe and Wiysonge, 2021). As vaccines became widely available, optimism grew regarding the crisis's resolution and the restoration of normal life and travel. Meanwhile, the strategic management of transportation restrictions, coupled with effective vaccine distribution, played a pivotal role in steering society back towards post-COVID normalcy.

Many mathematical models have been developed to demonstrate the spread and control of infectious disease. The topic of vaccine control and distribution are among the most heated ones (Müller, 1998). Vaccine distribution strategy involves systematically delivering and administering vaccines to target populations to prevent disease spread. During a pandemic, it is vital for achieving herd immunity and reducing transmission (Bonanni, 1999). An optimized

vaccination strategy cannot only improve the efficiency in reducing infections but also reduce the total cost associated with infection and vaccine administration, especially when vaccine supply is limited. Metapopulation-based epidemiology studies reveal the great influence of human mobility to pandemic control (Balcan et al., 2010; Chinazzi et al., 2020) and spatial vaccination strategies (Lemaitre et al., 2022). However, the study of simultaneous control for both transportation and vaccination, which involves the timing and level of implementing transportation-related interventions and vaccine source distribution, remains largely unexplored.

This study addresses this existing gap in the literature by formulating an optimization problem that centrally focuses on the joint optimization of transportation restrictions and vaccine distribution for the pandemic control considering spatial heterogeneities in mobility network and disease vulnerability. We consider the influence of both long- and short-distance transport to disease transmission in the model, while the transportation control is focused on long-distance mobility. This decision is based on the recognition that long-distance migration often facilitate rapid and extensive spread of infectious diseases across geographical boundaries, and they are relatively more manageable to regulate compared to short-range mobility. We formulate a nonlinear optimization problem focused on cost minimization, incorporating controls on an overall long-distance transportation rate and region-specific vaccination rates. The objective is to minimize the total cost associated with infection and interventions implementation, namely health and opportunity loss through infection, loss of income in tourism and transportation industries through travel restriction policies, and costs for acquiring and distributing vaccines. Our investigation also delves into the intricate dynamics of how vaccination impacts the optimal timing for easing transportation controls and, conversely, how transportation considerations influence the efficient distribution of vaccines. A susceptible-vaccinated-latent-infectious-removed (SVLIR) epidemic model is formulated within the metapopulation structure to account for both transportation and vaccination control variables. We apply Pontryagin's maximum principle to find the necessary conditions for our problem solution (Asano et al., 2008). A numerical experiment, using Japan's 2021 situation, is conducted to test the feasibility and effectiveness of our proposed model.

This study represents a novel strategy aimed at optimizing vaccine resource allocation and transport-related interventions for infectious disease management. By integrating demographic factors, transport economics, and real-world epidemiology data, it advocates for adaptive policy responses. Central to this strategy is fostering collaboration across various social sectors, emphasizing the importance of a unified approach to reducing cross-regional transmission through coordinated vaccine distribution and transportation restrictions.

The remainder of this paper is organized as follows. Section 2 furnishes a comprehensive literature review of pertinent studies. Section 3 introduces a modified metapopulation model and delineates the optimization problem concerning control measures. The simulation results of numerical experiments are presented in Section 4. Finally, Section 5 encapsulates the conclusions drawn from our findings and suggests various avenues for future research.

2. Literature Review

With the development of computational resources and data availability, there is a growing number of studies addressing the epidemic dynamics modelling and intervention analysis. Various epidemic models employ different fractional compartments to address many types of disease transmissibility (Chen et al., 2021). Their primary focus lies in predicting the outbreak patterns of infectious diseases and conducting associated risk assessments. While the intervention analysis addresses the optimization of implementation of control measures or the allocation and distribution of resources (Jordan et al., 2021). In this section, we offer a thorough review of epidemic dynamics modelling and optimization of intervention implementations.

Mainly two types of epidemic models have been categorized: agent-based models (Longini Jr et al., 2005; Ferguson et al., 2006; Ciofi degli Atti et al., 2008; Roche et al., 2011; Weiss, 2013) and metapopulation models (Colizza and Vespignani, 2008; Balcan et al., 2010; Chinazzi et al., 2020; Kraemer et al., 2020). The agent-based models represent the interactions among individuals that mediate disease transmission, while metapopulation models consider the spatial spread of infectious disease among different groups of population, within which individuals are well-mixed and homogeneous (Chowell et al., 2016). Therefore, highly-detailed individual interaction data and great computation power are needed in agent-based epidemic simulation (Vespignani et al., 2020), and structured metapopulation models require more extensive and complex sorts of data to estimate the parameters in different regions (Balcan et al., 2009).

Christley et al. (2005) indicated in the availability of interaction network and degree distribution, agent-based models enable the analysis of disease transmission pattern and provide valuable insights to intervention strategies.

However, the data complexity and computation cost limit the agent-based models from estimating the pandemic in global level (Ding et al., 2021). Metapopulation models group individuals into subpopulations and connect each subpopulation with mobility and transportation network (Colizza and Vespignani, 2008). The analysis of epidemic spreading can either be a regional level (Sattenspiel and Dietz, 1995; Lipshtat et al., 2021) or global level (Balcan et al., 2010; Chinazzi et al., 2020). Well-structured transportation and mobility network enables analysis of interventions associated with travel regulations (Luo et al., 2022; Liu et al., 2022; Nguyen et al., 2022; Liu et al., 2024), and lock-down and quarantine policies (Ding et al., 2021).

The control of vaccine administration is one of the most heated epidemic-related optimization problems (Biswas et al., 2014; Wang et al., 2019; Libotte et al., 2020; Moore et al., 2021), and research of vaccine control together with other pharmaceutical control measures such as prevention, screening, treatment, test, isolation are also well established (Kumar and Srivastava, 2017; Olivares and Staffetti, 2021; Shen et al., 2021; Khan et al., 2022). With the difference of vulnerability and influence of mobility network, vaccines are usually allocated with respect to age heterogeneity (Müller, 1998; Moore et al., 2021; Zhao et al., 2021) or spatial needs (Asano et al., 2008; Venkatramanan et al., 2017; Lemaitre et al., 2022; Caga-anan et al., 2023). The optimal control problems are mostly formulated as ordinary differential equations with an objective function and certain boundary conditions. By introducing adjoint variables (Lagrange multipliers), the Hamiltonian function can be formulated and optimal value of control variables can be determined by applying Pontryagin's maximum principle (Lenhart and Workman, 2007).

Transportation had played a critical role in the widespread of COVID-19 (Sun et al., 2021), such that the travel restriction policies (Liu and Yamamoto, 2022; Dantsuji et al., 2023), lockdown policies (Mars et al., 2022; Meng et al., 2022) and many others swiftly took place as efficacious control interventions. However, the analysis of optimal control of transportation for mitigating infection is not well extended. Ding et al. (2021) developed a decision-making framework to optimize the control of external connections between countries to address the transportation lock-down and quarantine problems. They combined different set of actions to minimize the social cost of lock-down and developed heuristic algorithm to find optimal solution from numerous discrete policy combinations. Luo et al. (2022) devised a trade-off mechanism for managing public transit as a sustainable response to the COVID-19 pandemic. They focused on the commute network in metapopulation structure and optimized the subway route operation to balance risks and economic benefit. Zhu et al. (2021) developed a sustainable border control policy by selectively permitting inbound tourists from other countries. Their policy also incorporates contact tracing and quarantine measures to mitigate the risks associated with border reopening.

Liu et al. (2024) established a relationship between disease transmission rate and long-distance mobility in a metapopulation-based SVLIR framework, and developed optimal tourism control strategy in a travel bubble framework. This previous study formulated a sequential decision problem to establish a discrete control for domestic and international transportation within the bubble-set countries. Our study builds upon the SVLIR framework by incorporating a novel region-specific vaccination control within the metapopulation structure to establish a control for both vaccination and transportation. We explore the spatial allocation of vaccine resource considering heterogeneities in mobility networks and epidemic vulnerability and examine the synergy effects between vaccination and transportation control interventions. Additionally, we employ optimal control methodologies devise continuous control mechanisms instead of discrete ones, enabling smoother and more precise adjustments to our strategy.

In summary, previous literature extensively explores optimization strategies for vaccination control and transportation management separately, but lacks integrated discussions covering both strategies. This gap in understanding hinders the recognition of synergy effects and effective resource incorporation. In transportation management, past studies predominantly favor discrete control methods over continuous ones, suggesting potential for enhanced flexibility and optimization. Additionally, there is a lack of development of a comprehensive transportation network that includes both local commuting and long-distance transport to optimize control strategies, resulting in potential drawbacks such as incomplete mitigation of transmission risks.

Our paper addresses the aforementioned research gap. To optimize vaccine distribution and transportation control simultaneously, we utilize a metapopulation model capturing spatial disease vulnerability and human mobility. Vaccine distribution control employs region-specific vaccination rates, while transportation control is represented by an overall transportation rate on long-distance transport, reducing mobility across subpopulations. Additionally, we incorporate disease transmission via commuting networks. By simulating epidemic dynamics, we minimize total costs through infection, controlled vaccine distribution and transportation reduction. Utilizing system control methodologies, we derive continuous control policies for both interventions. Results show significant reductions in infection and intervention resource input, with spatial differences observed in individual and concurrent control

Table 1: Summary of parameter descriptions.

Parameters	Description
S_j, V_j, L_j, I_j, R_j	Susceptible, vaccinated, latent, infectious, removed population in subpopulation j.
N_j	Population of subpopulation j, $N_j^{[m]}$ denotes compartment population, e.g., $N_j^{[S]} = S_j$.
κ_j	Daily contact rate of residents in j.
γ_S, γ_V	Infection rate among unvaccinated and vaccinated individuals.
β_j	Vaccination rate in j.
ξ	Rate of latency individuals turning to infectious.
ν	Rate of infectious individuals turning to removed.
$\boldsymbol{X}$	Long-distance transport matrix, X_{ij} denotes transport volume from i to j.
$\hat{\kappa}_j$	Adjusted daily contact rate with inbound tourists in j.
η	Coefficient of tourists' mobility.
α_j	Fraction of inbound tourists among all travelers arriving in j.
t_s	Average period of stay at destination during long-distance travel.
λ_j^S, λ_j^V	Effective infection force among susceptible and vaccinated individuals.
σ_{ij}	Commute rate from subpopulations i to j, $\sigma_i = \sum_j \sigma_{ij}$.
τ	Return rate of commuting individuals.
K	Number of subpopulations.
T	Number of discrete time periods.
δ	Transportation control variable.
J	Total cost of infection and intervention implementation.
$c^\delta, c_j^I, c^V, c_j^\beta$	Cost coefficients. Economy loss by transport control, infection cost, vaccine production or purchase cost, vaccine distribution cost, respectively.
P_j^{pop}	$P_j^{pop} = N_j/1,000$.
$\mu_{S,j}, \mu_{V,j}, \mu_{L,j}, \mu_{I,j}, \mu_{R,j}$	Adjoint variables associated with S_j, V_j, L_j, I_j, R_j.

measures.

3. Methodologies

In this section, we introduce the mathematic formulation of the metapopulation-based epidemic model with the effect of tourists' mobility adopted from Liu et al. (2024) in Subsection 3.1. The optimization control problem of vaccination and transportation control is proposed in Subsection 3.2 followed with the modified forward-backward sweep solution algorithm in Subsection 3.3. Please be noted that we provide a nomenclature table for all parameters in Table 1.

3.1. Metapopulation model

The disease transmission pattern in each subpopulation region is categorized as Susceptible-Vaccinated-Latent-Infecitous-Removed model, and illustrated in Fig. 1. Susceptible individuals can be infected at rate $\kappa\gamma_S$ or be vaccinated at rate β, where κ and γ_S denotes the contact rate of the subpopulation and the disease transmissibility among the unvaccinated people, respectively. Vaccinated individuals can also be infected at a lower rate of $\kappa\gamma_V$. Latent compartment comprises the people who are already infected but not yet infectious, with a latency period of ξ^{-1}. Infectious individuals can infect susceptible and vaccinated people and will progress to removed phase after ν^{-1}, during which they can no longer infect or be infected. The removed phase includes those are recovered, treated or deceased. The epidemic compartment transition dynamics is summarized in Eqs. (1) – (5) for each subpopulation j at time t:

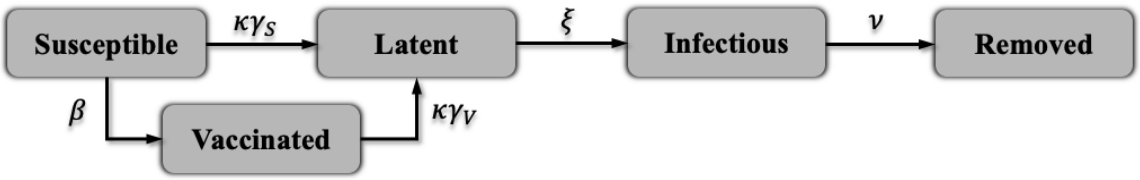

Figure 1: Epidemic compartment structure.

$$\Delta S_j/\Delta t = -\kappa_j\gamma_S I_j S_j/N_j - \beta_j S_j, \tag{1}$$
$$\Delta V_j/\Delta t = \beta_j S_j - \kappa_j\gamma_V I_j S_j/N_j, \tag{2}$$
$$\Delta L_j/\Delta t = \kappa_j I_j(\gamma_S S_j + \gamma_V V_j)/N_j - \xi L_j, \tag{3}$$
$$\Delta I_j/\Delta t = \xi L_j - \nu I_j, \tag{4}$$
$$\Delta R_j/\Delta t = \nu I_j. \tag{5}$$

Note that the use of contact rate κ is to verify the difference of infection speed in different regions considering the population density, gender and age structure and other factors.

With the long-distance transportation between subpopulations formulated as $\boldsymbol{X}(t)$, the compartment variation will become:

$$N_j^{[m]}(t+1) - N_j^{[m]}(t) = \Delta N_j^{[m]}(t) + \sum_i (X_{ij}^{[m]}(t) - X_{ji}^{[m]}(t)), \tag{6}$$

where $m \in \{S, V, L, I, R\}$. The formulation of $X_{ij}^{[m]}(t)$ is given by

$$X_{ij}^{[m]}(t) = X_{ij} p_i^{[m]}(t) = X_{ij}\frac{N_i^{[m]}(t)}{N_i}. \tag{7}$$

The tourists' mobility effect is reflected in the adjustment of local contact rate, summarized as $\hat{\kappa}_j$:

$$\hat{\kappa}_j = \mathcal{P}(\kappa_j, X_j(t)) = \kappa_j + (\eta - 1)\frac{\alpha_j t_s X_j(t)}{N_j}\kappa_j, \tag{8}$$

with the several tourism-related factors: tourist mobility coefficient η, fraction of inbound tourists among all travelers α_j and average duration of tourists' stay at the destination t_s.

Effective infection forces among susceptible and vaccinated individuals, λ_j^S and λ_j^V are formulated with local commuting rate σ_{ji} ($\sigma_j = \sum_i \sigma_{ji}$) and return rate of commuting τ:

$$\lambda_j^S = \frac{\lambda_{jj}^S}{1+\sigma_j/\tau} + \sum_i \frac{\lambda_{ji}^S \sigma_{ji}/\tau}{1+\sigma_j/\tau}, \tag{9}$$
$$\lambda_j^V = \frac{\lambda_{jj}^V}{1+\sigma_j/\tau} + \sum_i \frac{\lambda_{ji}^V \sigma_{ji}/\tau}{1+\sigma_j/\tau}, \tag{10}$$

where

$$\lambda_{jj}^S = \frac{\hat{\kappa}_j\gamma_S}{N_j}\left[\frac{I_j}{1+\sigma_j/\tau} + \sum_i \frac{I_i}{1+\sigma_i/\tau}\frac{\sigma_{ij}}{\tau}\right], \lambda_{ji}^S = \frac{\hat{\kappa}_i\gamma_S}{N_i}\left[\frac{I_i}{1+\sigma_i/\tau} + \sum_l \frac{I_l}{1+\sigma_l/\tau}\frac{\sigma_{li}}{\tau}\right],$$
$$\lambda_{jj}^V = \frac{\hat{\kappa}_j\gamma_V}{N_j}\left[\frac{I_j}{1+\sigma_j/\tau} + \sum_i \frac{I_i}{1+\sigma_i/\tau}\frac{\sigma_{ij}}{\tau}\right], \lambda_{ji}^V = \frac{\hat{\kappa}_i\gamma_V}{N_i}\left[\frac{I_i}{1+\sigma_i/\tau} + \sum_l \frac{I_l}{1+\sigma_l/\tau}\frac{\sigma_{li}}{\tau}\right].$$

Here we simply provide the formulations of the metapopulation-based epidemic model with the tourists' mobility effects for the need of mathematic structure and solution algorithm for our control problem. Readers can refer to the work of Balcan et al. (2010) and Liu et al. (2024) for detailed explanations.

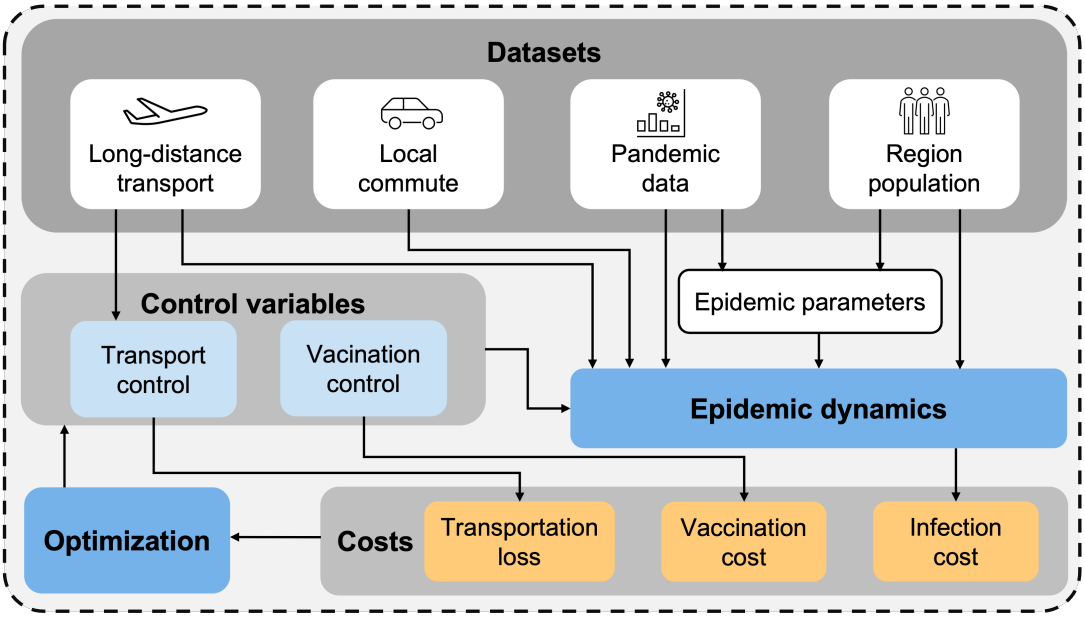

Figure 2: Research framework.

3.2. *Control problem*

A generalized research framework for the control optimization is illustrated in Fig. 2. The foundation of our epidemic modeling and control optimization is rooted in real data collection, including long-distance transport data, local commute data, historical pandemic data and demographic statistics. The long-distance transport includes air, railway, and cruise ship travel, which are cross-regional modes of travel. The local commute denotes travel to adjacent regions for school or work with regular returns. Long-distance transport and local commute are temporal travel matrices depicting population movements among subpopulations with different epidemic status. Historical pandemic data and demographic data are used to estimate epidemic parameters such as contact rate (intra-group mobility), real vaccination rate, population size, etc. We designate control variables to govern long-distance transport volumes and vaccination rates. The epidemic model use the input data and parameters to formulate the infection dynamics and calculate the total costs. By fine-tuning the control variables, we aim to minimize the total cost and identify optimal variable values.

The optimal control problem is designed to minimize the overall cost, encompassing losses in transportation, vaccination, and health, as well as opportunity loss resulting from infection. The control variables are represented as $\boldsymbol{\beta}(t) = (\beta_1(t), \beta_2(t), \cdots, \beta_K(t))$ for vaccination distribution across total K subpopulations, and $\delta(t)$ for the control of transportation among of the all subpopulations. Here, $\beta_j(t)$ $(j = 1, \cdots, K)$ denotes the proportion of individuals that are fully vaccinated relative to those susceptible (neither infected nor fully vaccinated). While, $\delta(t)$ is a measure of the current transportation volume as a fraction of the volume in an uncontrolled scenario, with $\delta(t)\boldsymbol{X}(t)$ signifying the actual transportation volume under imposed controls. This approach aligns with Lipshtat et al. (2021) to simulate transport limitations by proportionally scaling down all transportation with a single factor. We acknowledge that using a uniform control variable can be ambiguous in managing individual transport links. However, it provides a more straightforward and computationally feasible model for transport regulation. Our focus extends to a country-scale implementation, where subpopulation regions can symbolize administrative divisions. Each subpopulation undergoes vaccination at a specific rate, and all long-distance transportation is centrally regulated by policymakers to achieve system optimality.

With the transportation variation, the daily contact rate is reformulated as a function of δ denoting as

$$\hat{\kappa}_j(\delta) = \kappa_j + (\eta - 1)\frac{\alpha_j t_s \delta X_j(t)}{N_j}\kappa_j. \tag{11}$$

Eqs. (1) – (5) can be reformulated as

$$\frac{dS_j}{dt} = -(\lambda_j^S + \beta_j)S_j + \delta \sum_i (X_{ij}^S - X_{ji}^S), \tag{12}$$

$$\frac{dV_j}{dt} = -\lambda_j^V V_j + \beta_j S_j + \delta \sum_i (X_{ij}^V - X_{ji}^V), \tag{13}$$

$$\frac{dL_j}{dt} = -\xi L_j + \lambda_j^S S_j + \lambda_j^V V_j + \delta \sum_i (X_{ij}^L - X_{ji}^L), \tag{14}$$

$$\frac{dI_j}{dt} = -\nu I_j + \xi L_j + \delta \sum_i (X_{ij}^I - X_{ji}^I), \tag{15}$$

$$\frac{dR_j}{dt} = \nu I_j + \delta \sum_i (X_{ij}^R - X_{ji}^R). \tag{16}$$

The total cost function with control variables is formulated in Eq. (17), where c^δ denotes the coefficient of transportation control cost, c_j^I denotes the coefficient of health and opportunity loss associated with infection per 1,000 population, c^V as vaccine production or purchase cost and c_j^β as vaccine distribution cost:

$$J(\boldsymbol{\beta}, \delta) = \int_0^T \left\{ c^\delta (1-\delta)^2 + \sum_{j=1}^K \left[c_j^I \left(\frac{I_j}{P_j^{pop}} \right)^2 + c^V S_j \beta_j + c_j^\beta \beta_j^2 \right] \right\} dt. \tag{17}$$

The optimal control problem is denoted as the minimization of $J(\boldsymbol{\beta}, \delta)$ subject to the epidemic dynamics ordinary differential equations and bounded conditions for vaccination and transportation control:

$$\text{Problem } (\boldsymbol{P}): \begin{cases} \min J(\boldsymbol{\beta}, \delta) = \displaystyle\int_0^T \left\{ c^\delta (1-\delta)^2 + \sum_{j=1}^K \left[c_j^I \left(\frac{I_j}{P_j^{pop}} \right)^2 + c^V S_j \beta_j + c_j^\beta \beta_j^2 \right] \right\} dt, \\ s.t. \\ \quad \text{eq.}(12), (13), (14), (15), (16), & \forall j \in \{1, 2, \cdots, K\}, \forall t \in \{0, 1, \cdots, T\}, \\ \quad \beta_j(t) \in [\beta_j^{\min}, \beta_j^{\max}], & \forall j \in \{1, 2, \cdots, K\}, \forall t \in \{0, 1, \cdots, T\}, \\ \quad \delta(t) \in [\delta^{\min}, 1], & \forall t \in \{0, 1, \cdots, T\}, \\ \quad S_j(0), V_j(0), L_j(0), I_j(0), R_j(0), & \forall j \in \{1, 2, \cdots, K\}. \end{cases}$$

Hamiltonian function for problem $\boldsymbol{P}$ is given by

$$\begin{aligned} H(t, \boldsymbol{N}, \delta, \boldsymbol{\beta}) &= c^\delta (1-\delta)^2 + \sum_{j=1}^K \left[c_j^I \left(\frac{I_j}{P_j^{pop}} \right)^2 + c^V S_j \beta_j + c_j^\beta \beta_j^2 + \mu_{S,j} S'_j + \mu_{V,j} V'_j + \mu_{L,j} L'_j + \mu_{I,j} I'_j + \mu_{R,j} R'_j \right] \\ &= c^\delta (1-\delta)^2 + \sum_{j=1}^K \left\{ c_j^I \left(\frac{I_j}{P_j^{pop}} \right)^2 + c^V S_j \beta_j + c_j^\beta \beta_j^2 \right. \\ &\quad + \mu_{S,j} \left[-(\lambda_j^S + \beta_j) S_j + \delta \sum_i \left(X_{ij} \frac{S_i}{N_i} - X_{ji} \frac{S_j}{N_j} \right) \right] \\ &\quad + \mu_{V,j} \left[-\lambda_j^V V_j + \beta_j S_j + \delta \sum_i \left(X_{ij} \frac{V_i}{N_i} - X_{ji} \frac{V_j}{N_j} \right) \right] \\ &\quad + \mu_{L,j} \left[-\xi L_j + \lambda_j^S S_j + \lambda_j^V V_j + \delta \sum_i \left(X_{ij} \frac{L_i}{N_i} - X_{ji} \frac{L_j}{N_j} \right) \right] \\ &\quad + \mu_{I,j} \left[-\nu I_j + \xi L_j + \delta \sum_i \left(X_{ij} \frac{I_i}{N_i} - X_{ji} \frac{I_j}{N_j} \right) \right] \\ &\quad \left. + \mu_{R,j} \left[\nu I_j + \delta \sum_i \left(X_{ij} \frac{R_i}{N_i} - X_{ji} \frac{R_j}{N_j} \right) \right] \right\}. \end{aligned} \tag{18}$$

Here, $\boldsymbol{\mu}_{[m]} = (\mu_{[m],1}, \mu_{[m],2}, \cdots, \mu_{[m],K}), m \in \{S, V, L, I, R\}$ are adjoint variables associated with state variables S_j, V_j, L_j, I_j, R_j for all subpopulations $j \in \{1, 2, \cdots, K\}$.

The nonlinear complementarity problem for H is derived as

$$\mu'_{S,j} = -\frac{\partial H}{\partial S_j} = (\mu_{S,j} - \mu_{L,j})\lambda_j^S + (\mu_{S,j} - \mu_{V,j} - c^V)\beta_j - \frac{\delta}{N_j}\sum_i X_{ji}(\mu_{S,i} - \mu_{S,j}), \quad (19)$$

$$\mu'_{V,j} = -\frac{\partial H}{\partial V_j} = (\mu_{V,j} - \mu_{L,j})\lambda_j^V - \frac{\delta}{N_j}\sum_i X_{ji}(\mu_{V,i} - \mu_{V,j}), \quad (20)$$

$$\mu'_{L,j} = -\frac{\partial H}{\partial L_j} = (\mu_{L,j} - \mu_{I,j})\xi - \frac{\delta}{N_j}\sum_i X_{ji}(\mu_{L,i} - \mu_{L,j}), \quad (21)$$

$$\mu'_{I,j} = -\frac{\partial H}{\partial I_j} = (\mu_{I,j} - \mu_{R,j})\nu - \frac{2c_j^I I_j}{\left(P_j^{pop}\right)^2} + \sum_{m\in\{S,V\}}(\mu_{[m],j} - \mu_{L,j})N_j^{[m]}(\lambda_j^{[m]})_{I_j} - \frac{\delta}{N_j}\sum_i X_{ji}(\mu_{I,i} - \mu_{I,j}), \quad (22)$$

$$\mu'_{R,j} = -\frac{\partial H}{\partial R_j} = - \frac{\delta}{N_j}\sum_i X_{ji}(\mu_{R,i} - \mu_{R,j}), \quad (23)$$

where,

$$(\lambda_j^S)_{I_j} = \frac{\hat{\kappa}_j\gamma_S}{N_j}\frac{\tau^2}{(\tau+\sigma_j)^2} + \sum_i \frac{\hat{\kappa}_i\gamma_S}{N_i}\frac{\sigma_{ji}^2}{(\tau+\sigma_j)^2}, \quad (24)$$

$$(\lambda_j^V)_{I_j} = \frac{\hat{\kappa}_j\gamma_V}{N_j}\frac{\tau^2}{(\tau+\sigma_j)^2} + \sum_i \frac{\hat{\kappa}_i\gamma_V}{N_i}\frac{\sigma_{ji}^2}{(\tau+\sigma_j)^2}, \quad (25)$$

with the transversality conditions:

$$\mu_{S,j}(T) = \mu_{V,j}(T) = \mu_{L,j}(T) = \mu_{I,j}(T) = \mu_{R,j}(T) = 0. \quad (26)$$

Applying the Pontryagin's maximum principle, the optimality conditions for the control variables are given by

$$0 = \frac{\partial H}{\partial \beta_j^*} = c^V S_j + 2c_j^\beta \beta_j^* - \mu_{S,j}S_j + \mu_{V,j}S_j, \quad \forall j \in \{1, 2, \cdots, K\}, \quad (27)$$

$$0 = \frac{\partial H}{\partial \delta^*} = -2c^\delta(1-\delta) + \sum_{j=1}^K \left\{ \sum_{m\in\{S,V\}}(\mu_{L,j} - \mu_{[m],j})N_j^{[m]}(\lambda_j^{[m]})_\delta + \sum_{m\in\{S,V,L,I,R\}}\left[\mu_{[m],j}\sum_i\left(X_{ij}^{[m]} - X_{ji}^{[m]}\right)\right]\right\} \quad (28)$$

where

$$(\lambda_j^S)_\delta = \frac{(\eta-1)t_s\gamma_S}{1+\delta_j/\tau}\left[\frac{\alpha_j X_j \kappa_j}{N_j^2}\left(\frac{I_j}{1+\sigma_j/\tau} + \sum_i \frac{I_i\sigma_{ij}}{\tau+\sigma_i}\right) + \sum_i \frac{\alpha_i X_i \kappa_i}{N_i^2}\left(\frac{I_i}{1+\sigma_i/\tau} + \sum_l \frac{I_l\sigma_{li}}{\tau+\sigma_l}\right)\frac{\sigma_{ji}}{\tau}\right], \quad (29)$$

$$(\lambda_j^V)_\delta = \frac{(\eta-1)t_s\gamma_V}{1+\delta_j/\tau}\left[\frac{\alpha_j X_j \kappa_j}{N_j^2}\left(\frac{I_j}{1+\sigma_j/\tau} + \sum_i \frac{I_i\sigma_{ij}}{\tau+\sigma_i}\right) + \sum_i \frac{\alpha_i X_i \kappa_i}{N_i^2}\left(\frac{I_i}{1+\sigma_i/\tau} + \sum_l \frac{I_l\sigma_{li}}{\tau+\sigma_l}\right)\frac{\sigma_{ji}}{\tau}\right]. \quad (30)$$

Let

$$\Psi = \sum_{j=1}^K \left\{ \sum_{m\in\{S,V\}}(\mu_{L,j} - \mu_{[m],j})N_j^{[m]}(\lambda_j^{[m]})_\delta + \sum_{m\in\{S,V,L,I,R\}}\left[\mu_{[m],j}\sum_i\left(X_{ij}^{[m]} - X_{ji}^{[m]}\right)\right]\right\}. \quad (31)$$

Therefore, the problem $\boldsymbol{P}$ can be solved and the optimal value of control variables are given by

$$\beta_j^* = \min\left\{\max\left\{0, \frac{(\mu_{S,j} - \mu_{V,j} - c^V)S_j}{2c^\beta}\right\}, \beta_j^{\max}\right\}, \quad \forall j \in \{1, 2, \cdots, K\}, \quad (32)$$

$$\delta^* = \min\left\{\max\left\{0, 1 - \frac{\Psi}{2c^\delta}\right\}, 1\right\}. \quad (33)$$

3.3. Solution algorithm

We employ an adapted forward-backward sweep method (Lenhart and Workman, 2007) outlined in Algorithm 1 to solve the optimization problem. We select this method for its frequent utilization in epidemic modeling with optimization context, known for its simplicity in implementation and applicability to metapopulation models (Asano et al., 2008; Caga-anan et al., 2023). The convergence and stability of this method is confirmed by Hackbusch (1978). Within this algorithm, we implement a decreasing step size $z = 0.5/\sqrt{n+1}$ in each iteration n, ensuring convergence as we explore the optimal values for both control variables.

Algorithm 1 Forward-backward sweep method

1: **Initialize**: $\boldsymbol{N}(0)$, $\boldsymbol{\mu}(T) = \mathbf{0}$, convergence tolerance parameter $0 < \epsilon << 1$, initial feasible guess $\boldsymbol{\beta}^0$ and δ^0, $n := 0$, $r = +\infty$, $J^0 \leftarrow J(\boldsymbol{\beta}^0, \delta^0)$
2: **while** $r > \epsilon$ **do**
3: **for** $t = 1, \cdots, T$ **do**
4: obtain $\boldsymbol{N}^n(t)$ with $\{\, \boldsymbol{\beta}^n(t), \delta^n(t), \boldsymbol{N}^n(t-1) \,\}$ through Eqs. (12) – (16)
5: **end for**
6: **for** $t = T-1, \cdots, 0$ **do**
7: obtain $\boldsymbol{\mu}^n(t)$ with $\{\, \boldsymbol{\beta}^n(t), \delta^n(t), \boldsymbol{N}^n(t), \boldsymbol{\mu}^n(t+1) \,\}$ through Eqs. (19) – (23)
8: **end for**
9: $z \leftarrow 0.5/\sqrt{n+1}$
10: **for** $t = 1, \cdots, T$ **do**
11: **for** $j = 1, \cdots, K$ **do**
12: obtain $\bar{\beta}_j^{n+1}(t)$ with $\{\boldsymbol{N}^n(t), \boldsymbol{\mu}^n(t)\}$ through Eq. (32)
13: $\beta_j^{n+1}(t) \leftarrow (1-z) \cdot \beta_j^n(t) + z \cdot \bar{\beta}_j^{n+1}(t)$
14: **end for**
15: obtain $\bar{\delta}^{n+1}(t)$ with $\{\boldsymbol{N}^n(t), \boldsymbol{\mu}^n(t)\}$ through Eq. (33)
16: $\delta^{n+1}(t) \leftarrow (1-z) \cdot \delta^n(t) + z \cdot \bar{\delta}^{n+1}(t)$
17: **end for**
18: $J^{n+1} \leftarrow J(\boldsymbol{\beta}^{n+1}, \delta^{n+1})$
19: $r \leftarrow \left| J^{n+1} - J^n \right| / J^n$
20: $n \leftarrow n+1$
21: **end while**
22: **return** $\boldsymbol{\beta}^n$, δ^n, $\boldsymbol{N}^n$.

In this algorithm, the initial input of epidemic data $\boldsymbol{N}(0)$ for all subpopulations at the starting time is necessary. During each iteration, the epidemic dynamics of the entire time period are calculated using $\boldsymbol{N}(0)$ and the updated vaccination and transportation rate in the forward sweep (lines 3-4). Subsequently, with updated epidemic data, adjoint variables are obtained in the backward sweep (lines 6-7) by initializing $\boldsymbol{\mu}(T) = \mathbf{0}$. The vaccination rate and transportation rate are then refined with optimal conditions described in lines 10-16. Total cost is calculated with current control variables and epidemic condition, and the difference in total costs between iterations is compared. The iterative loop ceases when the difference in total costs between adjacent iterations falls below a predefined threshold ϵ ($r \leq \epsilon$).

This algorithm also presents an application for addressing the optimal vaccination and transportation control strategy independently. When seeking the optimal vaccination within a specified transportation control policy, we bypass lines 15 and 16 and modify line 18 to $J^{n+1} \leftarrow J(\boldsymbol{\beta}^{n+1}, \delta^0)$ in Algorithm 1. Similarly, we can skip lines 11-14 and change line 18 to $J^{n+1} \leftarrow J(\boldsymbol{\beta}^0, \delta^{n+1})$ to obtain a optimal control in transportation with a given vaccination distribution.

Unfortunately, there is no guarantee of convergence outcome for this algorithm when solving different problems with different scale or input parameters, especially with some many variables in the metapopulation structure. The selection of initial guess of control variables or step size z can greatly influence the convergence performance (Lenhart and Workman, 2007). In this study, we have carefully tested numerous combinations of initial guess and step size, ultimately found the decreasing step size $z = 0.5/\sqrt{n+1}$ demonstrated the best converge rate and speed across a range of initial guesses of control variables in our case study.

4. Numerical Experiments

To depict the optimal strategy of vaccination distribution and transportation control with our mathematic formulation, we conduct a numerical experiment focusing on Japan as the research subject. We partition Japan at the prefecture level into 47 subpopulation regions and simulate the epidemic dynamics in all regions over a 180-day period, commencing from July 1st, 2021. This specific timeframe is chosen as it coincided with the initiation of the second dose vaccine administration, and Japan was grappling with the fifth wave of infections (Lee et al., 2022). Table 2 summaries parameter values used in the simulation. In this experiment, we used the daily average transport volume of 2019 as our baseline for the uncontrolled scenario, encompassing transportation modes of airplanes, railways, and ships. The transport matrix $\boldsymbol{X}$ is visualized in two ways: as a transport connection map shown in Fig. 3(a), and as a heatmap in Fig. 3(b). From these illustrations, we can highlight the spatial heterogeneity in transportation and underscore the importance of an underlying transport network within the metapopulation structure. To approximate the actual transportation rate during the research period, we compare the mobile spatial data of the population residing outside their residential prefecture in 2021 and 2019 (NTT Docomo, 2023). Additionally, the actual vaccination rate (2 doses) and real infection data are sourced from SMU (2023), and contact rate κ in all prefectures is estimated based on the infection data, transportation and vaccination data we obtained.

Table 2: Parameter values in the experiment.

Parameters	Description	Value	Reference
γ_S	Infection rate among unvaccinated individuals	0.007	Liu and Ding (2022)
γ_V	Infection rate among vaccinated individuals	0.0002	Liu and Ding (2022)
ξ^{-1}	Latency period	5.5 (d^{-1})	Xin et al. (2022)
ν^{-1}	Infectious period	7 (d^{-1})	MHLW (2022)
σ	Commute rate between prefectures	-	Adachi et al. (2020)
τ	Return rate of commuting individuals	3 (d^{-1})	Balcan et al. (2010)
$\boldsymbol{X}$	Long-distance transport matrix	-	E-Stat (2023)
c^{δ}	Coefficient of economy loss by transport control	500260 (K$)	JTA (2022)
c_j^I	Coefficient of infection cost	$2 \times P_j^{pop}$ (K$)	Estimated
c^V	Vaccine production or purchase cost (2 doses)	0.041 (K$)	Mainichi (2023)
c_j^{β}	Vaccine distribution cost	-	Watanabe (2022)
η	Coefficient of tourist mobility	3	Estimated
t_s	Period of stay at destination of long-distance travel	1.8	JTA (2022)

In the numerical simulation, the initial inputs of variables, vaccination rate $\boldsymbol{\beta}^0$ and transport rate δ^0, are based on real historical data, serving as the base case scenario for our analysis. We establish the convergence tolerance at $\epsilon = 10^{-6}$, with the maximum vaccination rate $\beta^{\max}$ determined by the to-date maximum observed in the real vaccination rate, and a minimum vaccination rate set at 0.001. The transportation range is defined within $[0.5, 1]$. The initial state of our control system is the epidemic data in July 1st, 2021 for all prefectures in Japan. The forward-backward sweep algorithm is realized using Python programming language in Jupyter Notebook. For the experiment, we conduct three separate simulation scenarios using the methods described in Section 3.3: optimizing both vaccine distribution and transportation (OVT), optimizing only vaccine distribution (OV) and optimizing only transportation control (OT). In all three simulations, we maintain fixed external factors such as disease transmissibility, basic contact rate, population size, and cost coefficients, etc. Specifically, in the OV scenario, we set the transportation rate to actual historical data, while in the OT scenario, we fix the vaccination rate to real-world data. We obtain the simulation results of all three scenarios and analyze the differences between them.

Figure 4 illustrates the convergence performance of the simulations. In comparison to the base case, all three scenarios exhibit significant reductions in total cost: 31.6% (OVT), 18.1% (OV), and 17.2% (OT). The simulation results of transportation rate and overall vaccination rate are shown in Fig. 5 with compare to the real situation. The simulation period encounters the 4th SoE declared in July, 2021 started in Tokyo and later extended to other 17 prefectures (Okamoto, 2022), where a significant reduction in transportation is observed in the real transportation data. Fig. 5 depicts the outcomes of optimal control strategies across all scenarios. Subfigures (a) and (b) present the transportation rate and the cumulative transportation loss in the OVT and OT scenarios, respectively, as compared

to real-case data. Meanwhile, subfigures (c) and (d) demonstrate the combined vaccination rate and the cumulative vaccine administration in the OVT and OV scenarios, respectively, in comparison with historical data. In the transportation control results in Figs. 5 (a) and (b), we can observe that a much stricter control should be placed than the real situation in the first two and half months, while a gradual release takes place and the control ends at around day 120 in both OVT and OT. The simultaneous control of vaccination distribution can reduce the transportation control level and increase the cross-prefecture passenger count by 24 millions than the OT case over the simulation period.

In the vaccination control results illustrated in Figs. 5 (c) and (d), it is evident that the maximum rate is achieved within the first two months in both OVT and OV, followed with a smooth descending. The total vaccine count in OVT and OV is reduced by 20% compared to the real situation. The cumulative vaccine count in all prefectures are depicted in Fig. 6(a) where Tokyo, Kanagawa and Osaka require the most vaccine in controlling the infection in the OVT scenario. Although the difference in combined vaccination rate in all prefecture in OVT and OV is negligible, the box chart of vaccine count variation in prefectures in Fig. 6(b) indicates a redistribution of vaccine in OVT scenario compared to OV scenario within a range of $[-2.5\%, 1.5\%]$, totaling near 1 million doses. As is depicted in Fig. 6(c), prefectures with greater population and transportation volume are increased with vaccine requirement in OVT than OV. When compared to base case, all prefectures experience a reduction in the total vaccine requirement, with a decrease of up to 38.8% (OVT) and 37.2% (OV).

In the comparison to the base case simulation, the three optimized scenarios exhibit notable efficacy in reducing infections in Japan, as depicted in Fig. 7(a). In the initial months, the infection is observed to be higher in the scenario focusing solely on vaccination (OV) compared to that with only transportation control (OT). This difference can be attributed to the fact that while the vaccination rate in OV closely mirrors actual conditions, the transportation restrictions in OT are more stringent in the first two months, which accounts for the lower rate of infection observed in this scenario. As more vaccines are administered and transportation control are relaxed, OV experiences fewer infections than OT in the latter part. However, the optimization of vaccination distribution (OVT and OV) presents a higher infection count in the tail of the curve, primarily attributed to the considerably lower vaccination rate in the later period compared to the real situation.

Regarding the effectiveness of different control scenarios in each prefecture, Figs. 7(b) and (c) present box charts depicting the percentage reduction in cumulative infection and peak infection for the three scenarios compared to the base case. The overall reduction in cumulative infection for three scenarios are 12.8% (OVT), 6.3% (OV) and 9.4% (OT), while total reduction in peak infection count are 23.7%, 10.0% and 17.2%, respectively. The range of reduction of cumulative infection among all prefectures in OVT, OV and OT scenarios are [-2.7%, 22.3%], [-3.2%, 15.4%] and

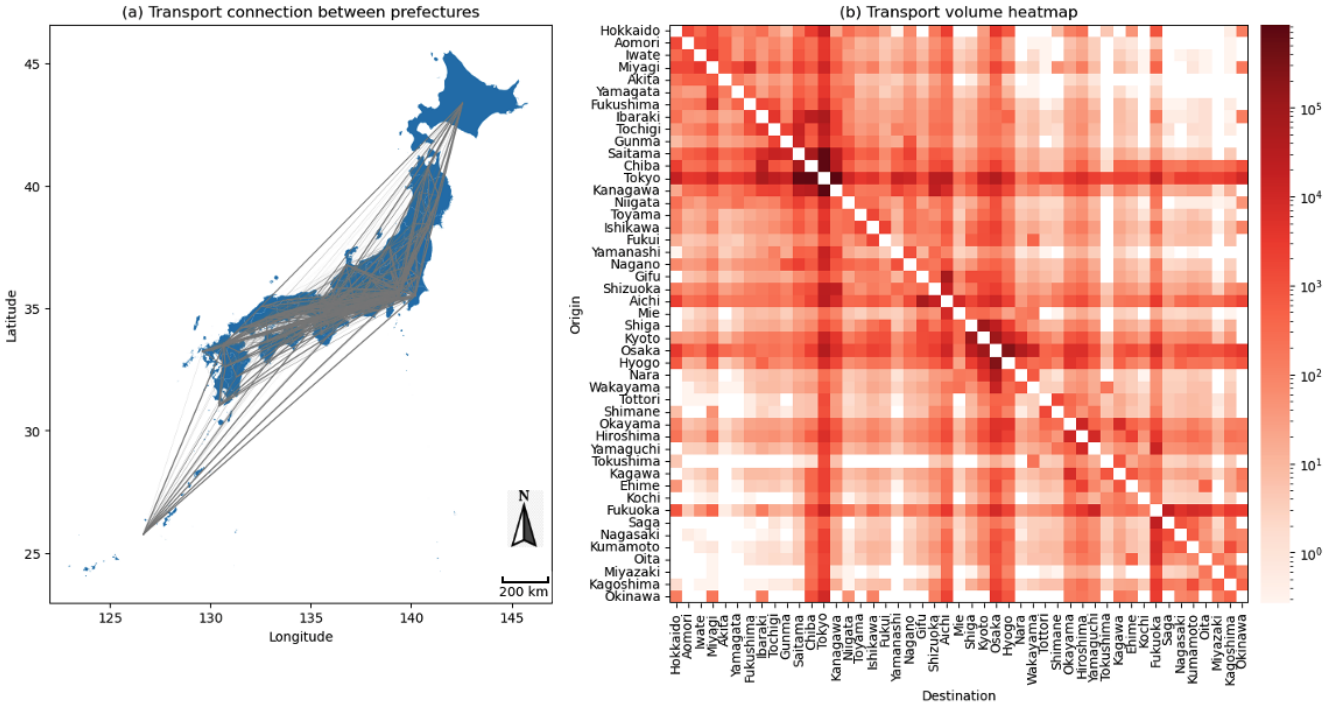

Figure 3: Long-distance transport between Japan prefectures.

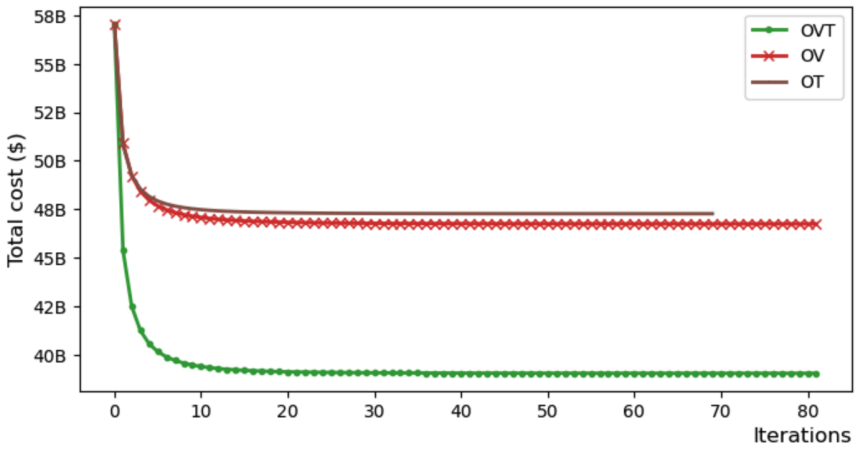

Figure 4: Convergence performance in experiment simulation.

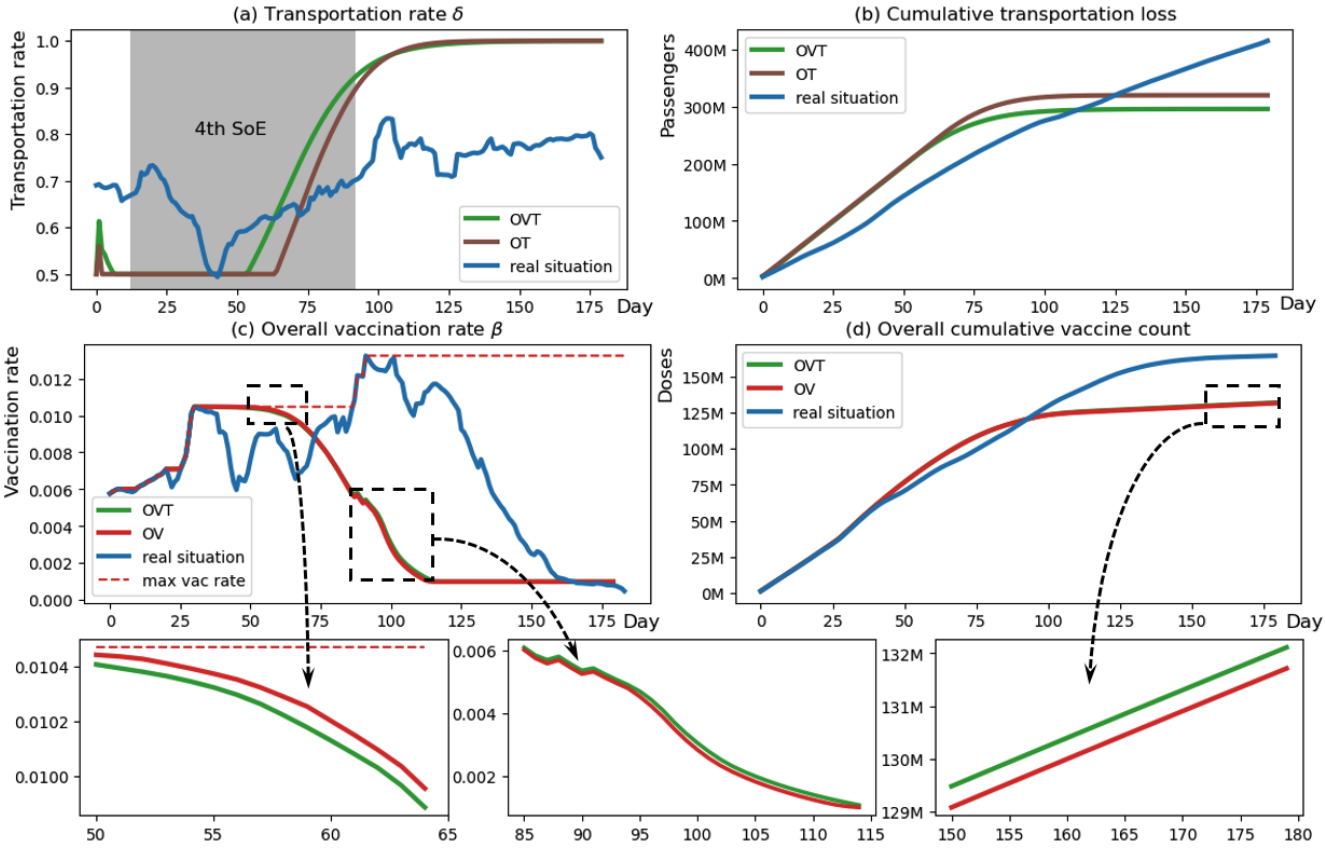

Figure 5: Simulation results of transportation and vaccination.

[0.7%, 13.3%], respectively. Meanwhile, the ranges of reduction of peak infection are [6.5%, 48.6%], [-6.7%, 40.9%] and [-0.7%, 22.5%], respectively. The reduction of cumulative and peak infection for all prefectures in Japan is visualized in Fig. 8. Two prefectures, Shimane and Tokushima, experience the increased cumulative infection in OVT and OV scenarios, attributed by the allocation of their vaccine to other regions, resulting in vaccinated populations in these two prefectures being among the lowest (37.6% and 41.6%, respectively) by the end. On the other hand, Akita, Nagasaki and Kumamoto show higher peak infections in the OV scenario because their real local vaccination rates in the beginning period are much larger than the national average and the maximum control rate, leading to smaller peak infection values in the base case compared to the optimized case (OV). Okinawa is the only prefecture with higher peak infection in OT than the base case. This can be attributed to the fraction of the peak infection population in the base case, which is 0.29% in Okinawa, only slightly smaller than the 0.32% in Tokyo. With lower transportation volume in Okinawa compared to Tokyo, the positive effect of transportation reduction is

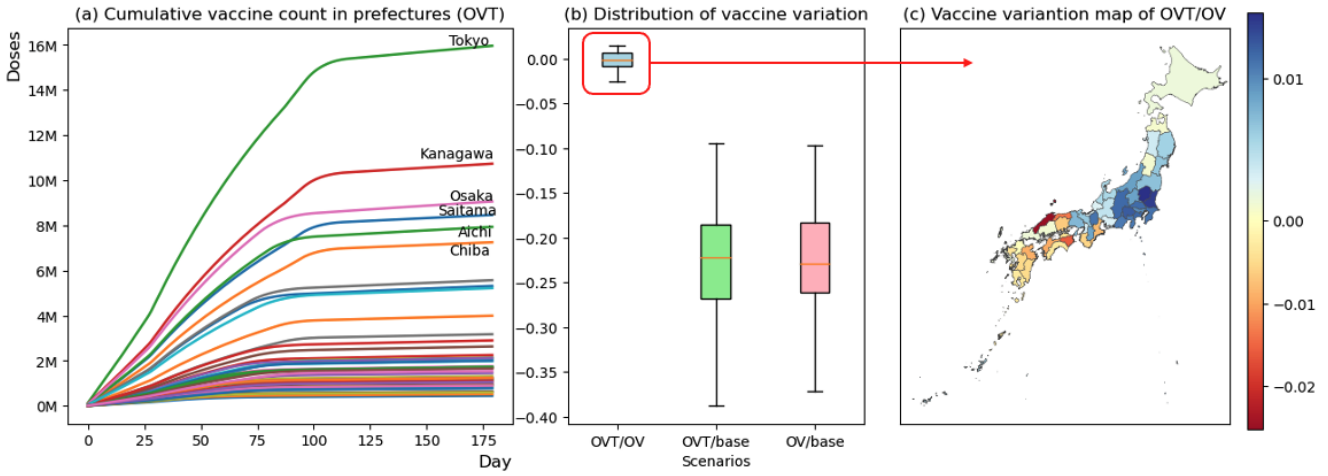

Figure 6: Vaccine distribution and variation by prefectures.

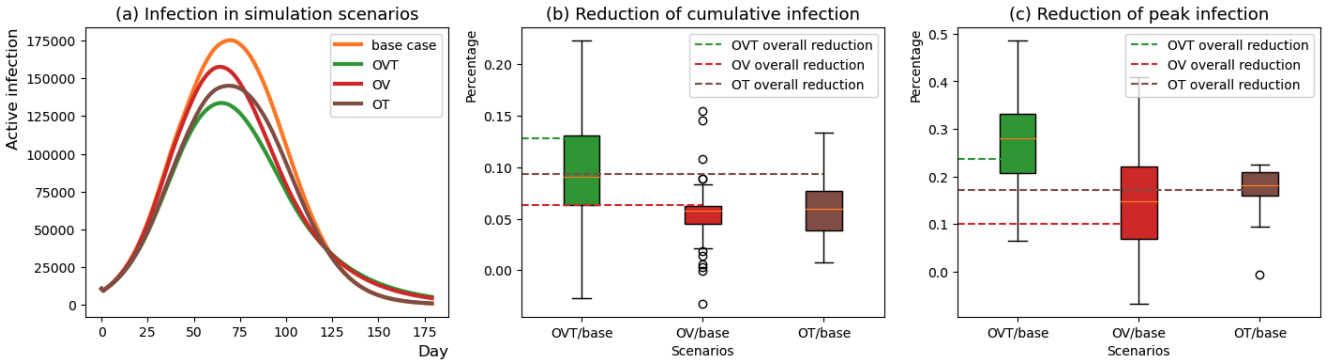

Figure 7: Simulation results of infection case count.

limited, resulting in the infectious population being mostly contained locally rather than spreading to other areas, further contributing to higher infection rates.

Interestingly, as is demonstrated in Fig. 8, transportation control exhibits its highest effectiveness in densely populated areas, notably in Kanto, Kansai, and Chubu. In contrast, vaccination control appears to be more susceptible in less populated areas. To quantify this observation, we calculate the standard deviation of the cumulative infection reduction across two groups of prefectures in the OVT case: the 24 less populated and the 24 more populated. The standard deviations are found to be 0.04 and 0.019, respectively, underscoring the differing impacts of these control measures based on population density. Although, within the current framework, we cannot identify key OD pairs within the transportation network, targeting transportation flow reductions specifically in regions like Kanto, Kansai and Chubu, while maintaining traffic levels elsewhere, may further minimize costs while maintaining effective pandemic control.

Through numerical experimentation, our model discerns spatial variations in mobility networks and epidemic vulnerability, revealing diverse responses among subpopulations to vaccination and transportation control measures. The observed reduction in total vaccination and less stringent transportation networks, coupled with improved epidemic conditions, shows the successful achievement of our strategy to minimize overall costs. The control strategies of transportation and vaccination both highlight its importance in reducing infection, and the simultaneous implementation of both measures is deemed most effective. By considering spatial nuances and leveraging the strengths of different interventions, the proposed strategy offers a holistic approach to pandemic control, emphasizing the importance of coordinated efforts tailored to each region's unique characteristics. It is critical to emphasize that transportation control and vaccination distribution, though distinct, interact synergistically in influencing pandemic control. An enhanced distribution of vaccines facilitates the earlier easing of transportation-related restrictions, while efficient transportation control ensures strategic allocation of vaccines to regions where they are most needed. This interplay underscores the importance of a holistic and integrated approach in optimizing pandemic management strategies.

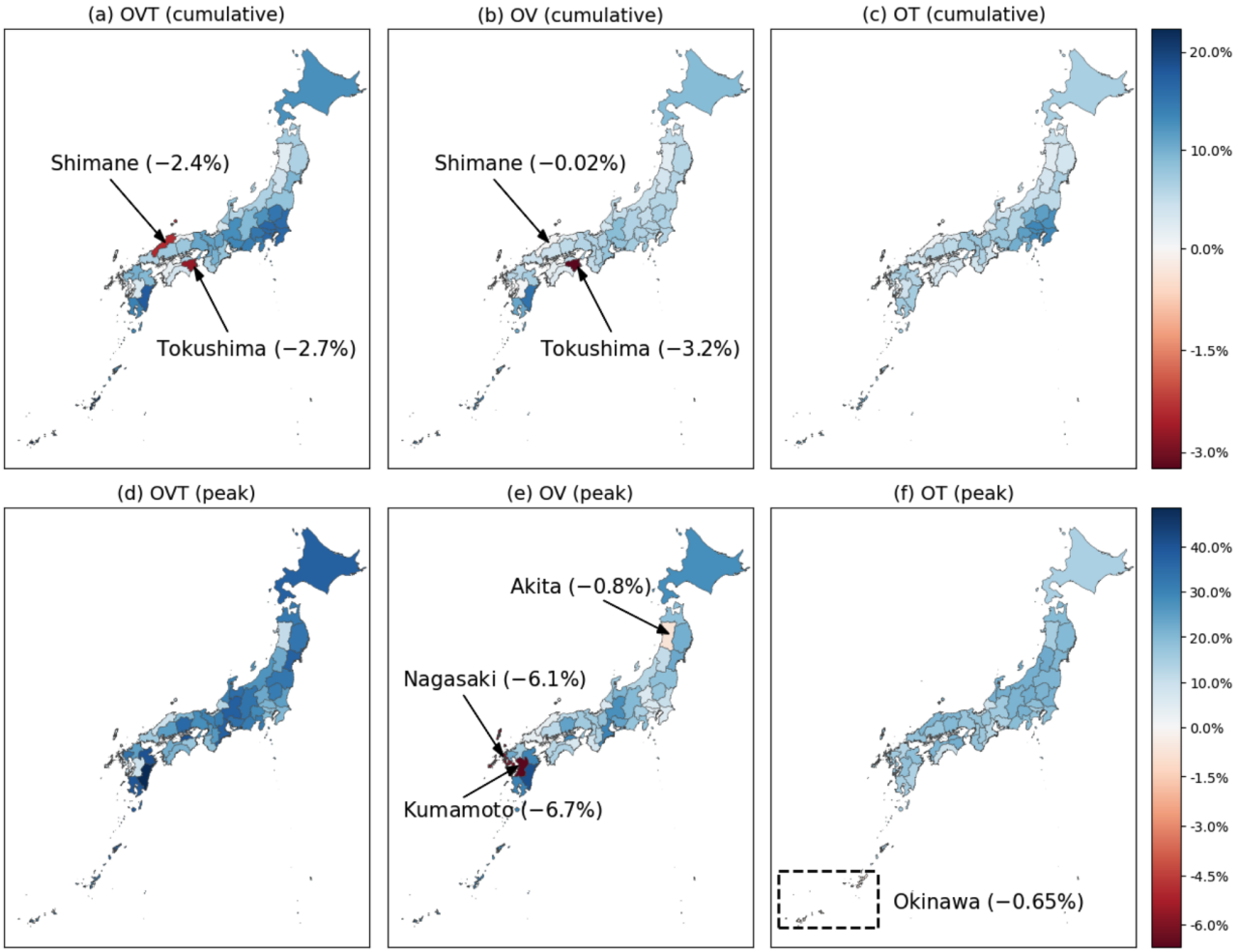

Figure 8: Heatmap of cumulative/peak infection reduction compared to base case.

The results also provide several key policy recommendations for managing pandemics effectively. Firstly, stricter transportation controls should be implemented immediately following the detection of an outbreak to limit the virus's spread. As vaccination coverage increases, these restrictions can be gradually eased, guided by vaccination benchmarks. Additionally, when vaccines become available, transportation restrictions should be coordinated with vaccination efforts. Depending on the vaccination progress in different regions, transportation can be lifted as early and as extensively as possible. Finally, policymakers must ensure clear communication and strict enforcement of transportation policies to achieve public compliance.

5. Conclusion

In conclusion, this study stems from the profound impact of the COVID-19 pandemic and the substantial societal costs associated with pandemic control measures. Our focus on optimizing two pivotal yet costly interventions—vaccination and transportation restrictions—aims to underscore the necessity of striking a careful balance for effective pandemic control. Within the framework of a metapopulation structure, we employ optimization strategies individually and concurrently, providing a detailed mathematical formulation with the application of Pontryagin's maximum principle. The case study in Section 4, centered on Japan, illustrates the considerable enhancements in infection control and cost reduction achievable through our optimization approach.

Our optimization framework demonstrates that achieving superior pandemic control across the entire country requires fewer vaccines and less stringent transportation control. While some regions may experience a marginal increase in infections with optimized strategies, this rise in the infectious population is outweighed significantly by reduced infections in other regions. A more effective vaccination strategy enables an increase in transportation volume for 24 million passengers in Japan over a six-month period. Additionally, the optimization of transportation necessitates the allocation of nearly 1 million vaccine doses. Notably, our findings highlight the varying effectiveness

of vaccination and transportation control in different regions, with populated areas more impacted by transportation control and less populated areas more susceptible to vaccination strategy effects.

This study pioneers the optimization control of non-pharmaceutical and pharmaceutical interventions during a global pandemic and offers a foundation for policymakers to develop more nuanced and effective strategies for future health crises. We emphasize the importance of incorporating spatial considerations into policy implementation for tailored strategies and effective pandemic control. The research structure also offers several key contributions to policy development in managing infectious diseases within matepopulations. Firstly, it contributes to optimized resource allocation by identifying key demographic epidemiology factors and considering transport economics, striking a balance between infection control and economic recovery. Secondly, it facilitates targeted intervention strategies by understanding how transportation networks contribute to disease spread, enabling policymakers to implement measures in different areas. Additionally, it advocates for adaptive policy responses, emphasizing the need for flexible frameworks based on real-data collection. Lastly, the extension of the framework to worldwide level can help understand the importance of international collaboration in coordinating vaccine distribution and transportation restrictions across borders to reduce cross-border transmission.

It is important to acknowledge certain limitations of our study. Firstly, our model relies on certain assumptions about disease transmission and human behavior, which might not capture the full complexity of real-world scenarios. The effectiveness of control measures can be influenced by factors like public compliance and vaccine efficacy, which were not explicitly modeled in our study. Secondly, A uniform transport control variable serves as a rapid implementation of measures during the early stages of a pandemic and acts as an initial assumption to analyze the overall impact of transportation reduction policies. In future studies, this approach can be further refined to develop more detailed and link-specific transportation control strategies. We also highlight the potential for future research to focus on identifying critical OD pairs within transportation networks by extending the current framework. With concentrating efforts on these key routes, policymakers can more effectively allocate resources, leading to more efficient and effective pandemic management. Thirdly, short-range transportation such as subway, bus and private car, is also critical in the spread of epidemic. We acknowledge that a comprehensive approach to disease management must also address the complexities of short-range travel within matepopulations. Future research endeavors should explore strategies for integrating both long and short-range transport control measures to enhance overall disease containment efforts. Additionally, the difference of various transport modes are not distinguished in the current research, future works can enhancing the characterization of transportation networks and devising multiple control strategies for multimodal transport systems. As our analysis extends globally, countries reach an equilibrium state as they compete for vaccine resources, and factors influencing vaccine export or import become critical in shaping the global transportation structure. Future research endeavors can delve into these aspects, expanding the scope of analysis and providing a more comprehensive understanding of optimal pandemic control strategies on a global scale.

Acknowledgements

We are grateful for the financial support of the Japan Science and Technology Agency, the establishment of university fellowships towards the creation of science technology innovation, Grant Number JPMJFS2112.

References

Adachi, D., Fukai, T., Kawaguchi, D., and Saito, Y. U. (2020). Commuting zones in Japan. *Research Institute of Economy, Trade and Industry (RIETI) Discussion Paper*.

Asano, E., Gross, L. J., Lenhart, S., and Real, L. A. (2008). Optimal control of vaccine distribution in a rabies metapopulation model. *Mathematical Biosciences and Engineering*, 5(2):219–238.

Balcan, D., Colizza, V., Gonçalves, B., Hu, H., Ramasco, J. J., and Vespignani, A. (2009). Multiscale mobility networks and the spatial spreading of infectious diseases. *Proceedings of the National Academy of Sciences*, 106(51):21484–21489.

Balcan, D., Gonçalves, B., Hu, H., Ramasco, J. J., Colizza, V., and Vespignani, A. (2010). Modeling the spatial spread of infectious diseases: The GLobal Epidemic and Mobility computational model. *Journal of Computational Science*, 1(3):132–145.

Biswas, M. H. A., Paiva, L. T., and de Pinho, M. D. R. (2014). A SEIR model for control of infectious diseases with constraints. *Mathematical Biosciences and Engineering*, 11(4):761–784.

Bonanni, P. (1999). Demographic impact of vaccination: a review. *Vaccine*, 17:S120–S125.

Caga-anan, R. L., Macalisang, J. M., Dalisay, J. L. M., Raza, M. N., Martinez, J. G. T., and Arcede, J. P. (2023). Optimal vaccination control for COVID-19 in a metapopulation model: A case of the Philippines. *Frontiers in Applied Mathematics and Statistics*, 9:1154634.

Chen, Y., Liu, F., Yu, Q., and Li, T. (2021). Review of fractional epidemic models. *Applied Mathematical Modelling*, 97:281–307.

Chinazzi, M., Davis, J. T., Ajelli, M., Gioannini, C., Litvinova, M., Merler, S., Pastore y Piontti, A., Mu, K., Rossi, L., Sun, K., Viboud, C., Xiong, X., Halloran, M. E., Longini jr., I. M., and Vespignani, A. (2020). The effect of travel restrictions on the spread of the 2019 novel coronavirus (COVID-19) outbreak. *Science*, 368(6489):395–400.

Chowell, G., Sattenspiel, L., Bansal, S., and Viboud, C. (2016). Mathematical models to characterize early epidemic growth: A review. *Physics of Life Reviews*, 18:66–97.

Christley, R. M., Pinchbeck, G., Bowers, R. G., Clancy, D., French, N. P., Bennett, R., and Turner, J. (2005). Infection in social networks: Using network analysis to identify high-risk individuals. *American Journal of Epidemiology*, 162(10):1024–1031.

Ciofi degli Atti, M. L., Merler, S., Rizzo, C., Ajelli, M., Massari, M., Manfredi, P., Furlanello, C., Scalia Tomba, G., and Iannelli, M. (2008). Mitigation measures for pandemic influenza in Italy: An individual based model considering different scenarios. *PloS One*, 3(3):e1790.

Colizza, V. and Vespignani, A. (2008). Epidemic modeling in metapopulation systems with heterogeneous coupling pattern: Theory and simulations. *Journal of Theoretical Biology*, 251(3):450–467.

Dantsuji, T., Sugishita, K., and Fukuda, D. (2023). Understanding changes in travel patterns during the COVID-19 outbreak in the three major metropolitan areas of Japan. *Transportation Research Part A: Policy and Practice*, 175:103762.

Ding, Y., Wandelt, S., and Sun, X. (2021). TLQP: Early-stage transportation lock-down and quarantine problem. *Transportation Research Part C: Emerging Technologies*, 129:103218.

Dube, K., Nhamo, G., and Chikodzi, D. (2021). COVID-19 pandemic and prospects for recovery of the global aviation industry. *Journal of Air Transport Management*, 92:102022.

E-Stat (2023). Freight regional mobility survey and passenger regional mobility survey. https://www.e-stat.go.jp/stat-search/files?tclass=000001056011&cycle=8&year=20211. (Accessed on December 15, 2023).

Ferguson, N. M., Cummings, D. A., Fraser, C., Cajka, J. C., Cooley, P. C., and Burke, D. S. (2006). Strategies for mitigating an influenza pandemic. *Nature*, 442(7101):448–452.

Hackbusch, W. (1978). A numerical method for solving parabolic equations with opposite orientations. *Computing*, 20(3):229–240.

Hale, T., Cameron-Blake, E., Folco, M. d., Furst, R., Green, K., Phillips, T., Sudarmawan, A., Tatlow, H., and Zha, H. (2022). What have we learned from tracking every government policy on COVID-19 for the past two years. *BSG Research Note*.

Jordan, E., Shin, D. E., Leekha, S., and Azarm, S. (2021). Optimization in the context of COVID-19 prediction and control: A literature review. *IEEE Access*, 9:130072–130093.

JTA (2022). White paper on tourism in Japan, 2022 (summary). Technical report, Japan Tourism Agency. https://www.mlit.go.jp/kankocho/en/siryou/content/001583966.pdf. (Accessed on December 15, 2023).

Khan, A. A., Ullah, S., and Amin, R. (2022). Optimal control analysis of COVID-19 vaccine epidemic model: A case study. *The European Physical Journal Plus*, 137(1):1–25.

Kraemer, M. U., Yang, C.-H., Gutierrez, B., Wu, C.-H., Klein, B., Pigott, D. M., Open COVID-19 Data Working Group, Du Plessis, L., Faria, N. R., Li, R., Hanage, W. P., Brownstein, J. S., Layan, M., Vespignani, A., Tian, H., Dye, C., Pybus, O. G., and Scarpino, S. V. (2020). The effect of human mobility and control measures on the COVID-19 epidemic in China. *Science*, 368(6490):493–497.

Kumar, A. and Srivastava, P. K. (2017). Vaccination and treatment as control interventions in an infectious disease model with their cost optimization. *Communications in Nonlinear Science and Numerical Simulation*, 44:334–343.

Lee, H., Chubachi, S., Namkoong, H., Asakura, T., Tanaka, H., Otake, S., Nakagawara, K., Morita, A., Fukushima, T., Watase, M., Kusumoto, T., Masaki, K., Kamata, H., Ishii, M., Hasegawa, N., Harada, N., Ueda, T., Ueda, S., Ishiguro, T., Arimura, K., Saito, F., Yoshiyama, T., Nakano, Y., Mutoh, Y., Suzuki, Y., Murakami, K., Okada, Y., Koike, R., Kitagawa, Y., Kimura, A., Imoto, S., Miyano, S., Ogawa, S., Kanai, T., and Fukunaga, K. (2022). Characteristics of hospitalized patients with COVID-19 during the first to fifth waves of infection: A report from the Japan COVID-19 task force. *BMC Infectious Diseases*, 22(1):935.

Lemaitre, J. C., Pasetto, D., Zanon, M., Bertuzzo, E., Mari, L., Miccoli, S., Casagrandi, R., Gatto, M., and Rinaldo, A. (2022). Optimal control of the spatial allocation of COVID-19 vaccines: Italy as a case study. *PLoS Computational Biology*, 18(7):e1010237.

Lenhart, S. and Workman, J. T. (2007). *Optimal control applied to biological models*. CRC Press.

Libotte, G. B., Lobato, F. S., Platt, G. M., and Neto, A. J. S. (2020). Determination of an optimal control strategy for vaccine administration in COVID-19 pandemic treatment. *Computer Methods and Programs in Biomedicine*, 196:105664.

Lipshtat, A., Alimi, R., and Ben-Horin, Y. (2021). Commuting in metapopulation epidemic modeling. *Scientific Reports*, 11:15198.

Liu, J., Ong, G. P., and Pang, V. J. (2022). Modelling effectiveness of COVID-19 pandemic control policies using an area-based SEIR model with consideration of infection during interzonal travel. *Transportation Research Part A: Policy and Practice*,

161:25–47.
Liu, S. and Yamamoto, T. (2022). Role of stay-at-home requests and travel restrictions in preventing the spread of COVID-19 in Japan. *Transportation Research Part A: Policy and Practice*, 159:1–16.
Liu, X. and Ding, Y. (2022). Stability and numerical simulations of a new SVIR model with two delays on COVID-19 booster vaccination. *Mathematics*, 10(10):1772. http://doi.org/10.3390/math10101772.
Liu, Y., Hanaoka, S., and Sugishita, K. (2024). Decision-making of travel bubble implementation process using metapopulation model. *Journal of the Air Transport Research Society*, 2:100009.
Longini Jr, I. M., Nizam, A., Xu, S., Ungchusak, K., Hanshaoworakul, W., Cummings, D. A., and Halloran, M. E. (2005). Containing pandemic influenza at the source. *Science*, 309(5737):1083–1087.
Luo, Q., Gee, M., Piccoli, B., Work, D., and Samaranayake, S. (2022). Managing public transit during a pandemic: The trade-off between safety and mobility. *Transportation Research Part C: Emerging Technologies*, 138:103592.
Mainichi (2023). Over 77.8 million COVID vaccine doses dumped in Japan, worth an estimate $1.6 billion. https://mainichi.jp/english/articles/20230318/p2a/00m/0na/010000c. (Accessed on December 18, 2023).
Mars, L., Arroyo, R., and Ruiz, T. (2022). Mobility and wellbeing during the COVID-19 lockdown. Evidence from Spain. *Transportation Research Part A: Policy and Practice*, 161:107–129.
Meng, X., Guo, M., Gao, Z., Yang, Z., Yuan, Z., and Kang, L. (2022). The effects of wuhan highway lockdown measures on the spread of COVID-19 in China. *Transport Policy*, 117:169–180.
MHLW (2022). Handbook of health and welfare statistics 2022. https://www.mhlw.go.jp/english/database/db-hh/2-2.html. (Accessed on June 30, 2023).
Moore, S., Hill, E. M., Dyson, L., Tildesley, M. J., and Keeling, M. J. (2021). Modelling optimal vaccination strategy for SARS-CoV-2 in the UK. *PLoS Computational Biology*, 17(5):e1008849.
Müller, J. (1998). Optimal vaccination patterns in age-structured populations. *SIAM Journal on Applied Mathematics*, 59(1):222–241.
Murano, Y., Ueno, R., Shi, S., Kawashima, T., Tanoue, Y., Tanaka, S., Nomura, S., Shoji, H., Shimizu, T., Nguyen, H., Miyata, H., Gilmour, S., and Yoneoka, D. (2021). Impact of domestic travel restrictions on transmission of COVID-19 infection using public transportation network approach. *Scientific Reports*, 11(1):3109.
Ndwandwe, D. and Wiysonge, C. S. (2021). COVID-19 vaccines. *Current Opinion in Immunology*, 71:111–116.
Nguyen, T. K., Hoang, N. H., Currie, G., and Vu, H. L. (2022). Enhancing COVID-19 virus spread modeling using an activity travel model. *Transportation Research Part A: Policy and Practice*, 161:186–199.
NTT Docomo (2023). Mobile spatial statistics. https://mobaku.jp. (Accessed on December 18, 2023).
Okamoto, S. (2022). State of emergency and human mobility during the COVID-19 pandemic in Japan. *Journal of Transport & Health*, 26:101405.
Olivares, A. and Staffetti, E. (2021). Optimal control-based vaccination and testing strategies for COVID-19. *Computer Methods and Programs in Biomedicine*, 211:106411.
Roche, B., Drake, J. M., and Rohani, P. (2011). An agent-based model to study the epidemiological and evolutionary dynamics of Influenza viruses. *BMC Bioinformatics*, 12:1–10.
Sattenspiel, L. and Dietz, K. (1995). A structured epidemic model incorporating geographic mobility among regions. *Mathematical Biosciences*, 128(1-2):71–91.
Shen, Z.-H., Chu, Y.-M., Khan, M. A., Muhammad, S., Al-Hartomy, O. A., and Higazy, M. (2021). Mathematical modeling and optimal control of the COVID-19 dynamics. *Results in Physics*, 31:105028.
SMU (2023). The trend of new coronavirus infection cases per capita. Sapporo Medical University. https://web.sapmed.ac.jp/canmol/coronavirus/index.html. (Accessed on December 18, 2023).
Sun, X., Wandelt, S., and Zhang, A. (2021). Delayed reaction towards emerging COVID-19 variants of concern: Does history repeat itself? *Transportation Research Part A: Policy and Practice*, 152:203–215.
UNWTO (2020). New data shows impact of COVID-19 on tourism as UNWTO calls for responsible restart of the sector. https://www.unwto.org/news/new-data-shows-impact-of-covid-19-on-tourism. (Accessed on June 30, 2023).
Venkatramanan, S., Chen, J., Gupta, S., Lewis, B., Marathe, M., Mortveit, H., and Vullikanti, A. (2017). Spatio-temporal optimization of seasonal vaccination using a metapopulation model of influenza. In *2017 IEEE International Conference on Healthcare Informatics (ICHI)*, pages 134–143. IEEE.
Vespignani, A., Tian, H., Dye, C., Lloyd-Smith, J. O., Eggo, R. M., Shrestha, M., Scarpino, S. V., Gutierrez, B., Kraemer, M. U., Wu, J., Leung, K., and M., L. G. (2020). Modelling COVID-19. *Nature Reviews Physics*, 2(6):279–281.
Wang, X., Peng, H., Shi, B., Jiang, D., Zhang, S., and Chen, B. (2019). Optimal vaccination strategy of a constrained time-varying SEIR epidemic model. *Communications in Nonlinear Science and Numerical Simulation*, 67:37–48.
Watanabe, K. (2022). Regarding the supplementary budget for fiscal year 2021 and the budget for fiscal year 2022. Technical report, Ministry of Finance, Government of Japan. https://www.mof.go.jp/public_relations/finance/202202/202202c.pdf. (Accessed on December 15, 2023).
Weiss, H. H. (2013). The SIR model and the foundations of public health. *Materials matematics*, pages 0001–17.
Xin, H., Li, Y., Wu, P., Li, Z., Lau, E. H., Qin, Y., Wang, L., Cowling, B. J., Tsang, T. K., and Li, Z. (2022). Estimating the latent period of coronavirus disease 2019 (COVID-19). *Clinical Infectious Diseases*, 74(9):1678–1681.

Zhang, J., Zhang, R., Ding, H., Li, S., Liu, R., Ma, S., Zhai, B., Kashima, S., and Hayashi, Y. (2021). Effects of transport-related COVID-19 policy measures: A case study of six developed countries. *Transport Policy*, 110:37–57.

Zhao, Z., Niu, Y., Luo, L., Hu, Q., Yang, T., Chu, M., Chen, Q., Lei, Z., Rui, J., Song, C., Lin, S., Wang, Y., Xu, J., Zhu, Y., Liu, X., Yang, M., Huang, J., Liu, W., Deng, B., Liu, C., Li, Z., Li, P., Su, Y., Zhao, B., Huang, W., Frutos, R., and Chen, T. (2021). The optimal vaccination strategy to control COVID-19: A modeling study in Wuhan city, China. *Infectious Diseases of Poverty*, 10(06):48–73.

Zhu, Z., Weber, E., Strohsal, T., and Serhan, D. (2021). Sustainable border control policy in the COVID-19 pandemic: A math modeling study. *Travel Medicine and Infectious Disease*, 41:102044.